2-Phenyl-4-quinolone (YT-1) induces G_2/M phase arrest and an intrinsic apoptotic mechanism in human leukemia cells

MENG-WEI LIN[1*], JAI-SING YANG[2*], CHI-CHENG LU[3], CHINGJU LIN[4], SHENG-CHU KUO[5], FUU-JEN TSAI[6-8] and MIAU-RONG LEE[9]

[1]Department of Nursing, Cardinal Tien Junior College of Healthcare and Management, New Taipei 231; [2]Department of Medical Research, China Medical University Hospital, China Medical University, Taichung 404; [3]Department of Pharmacy, Buddhist Tzu Chi General Hospital, Hualien 970; [4]Department of Physiology, and [5]School of Pharmacy, China Medical University; [6]Genetics Center, Department of Medical Research, China Medical University Hospital; [7]School of Chinese Medicine, China Medical University; [8]Department of Medical Genetics, China Medical University Hospital; [9]Department of Biochemistry, China Medical University, Taichung 404, Taiwan, R.O.C.

Received July 31, 2017; Accepted December 12, 2017

DOI: 10.3892/or.2017.6170

Abstract. The present study aimed to investigate the biological effects of the new compound 2-phenyl-4-quinolone (YT-1) on human leukemia cells. Cell viability was determined by propidium iodide (PI) exclusion method followed by flow cytometry. Our results showed that YT-1 inhibited the cell viability and resulted in morphologic changes to the U937, HL-60 and K562 cells, respectively. Among them, U937 cells were the most sensitive cell line. On the contrary, YT-1 had no cytotoxic effects on human fetal skin fibroblast WS1 cells. Flow cytometric analysis indicated that YT-1 induced G_2/M phase arrest and apoptosis (sub-G1 population) in U937 cells. The presence of apoptotic bodies evidenced by DAPI staining and DNA fragmentation detected by agarose gel electrophoresis further supported the induction of apoptosis in the YT-1-treated U937 cells. Annexin V/PI staining of U937 cells confirmed that the early apoptotic event occurred after YT-1 exposure. YT-1 disrupted the mitochondrial membrane potential ($\Delta\Psi m$) in a time-dependent manner. YT-1 increased the protein levels of Bax and Bak but decreased Bcl-2 and Bid protein levels in U937 cells in a time-dependent manner. In addition, YT-1 stimulated the expression of cytochrome *c* and proteolytic activation of caspase-3 and caspase-9 after exposure to YT-1 in U937 cells. In summary, YT-1 suppressed the viability of U937 leukemia cells through the intrinsic apoptosis pathway. YT-1 is a potential chemotherapeutic candidate for the treatment of leukemia.

Correspondence to: Dr Miau-Rong Lee, Department of Biochemistry, China Medical University, 91 Hsueh-Shih Road, Taichung 404, Taiwan, R.O.C.
E-mail: mrlee@mail.cmu.edu.tw

*Contributed equally

Key words: YT-1, G_2/M phase, apoptosis, leukemia cells

Introduction

Leukemia is one of the most common hematological malignancies in humans (1,2). Chemotherapy, target therapy, radiotherapy and hematopoietic stem cell (HSC) transplantation are common therapies for leukemia (3,4). However, chemoresistance and severe side-effects caused by high-dose chemotherapy drugs are current hurdles to effective treatment (5,6). Therefore, the screening of target-specific small-molecule drugs for leukemia treatment is crucial.

2-Phenyl-4-quinolone derivatives have various pharmacological effects including anti-inflammatory and anticancer activities (7-10). We have designed and synthesized a new series of 2-phenyl-4-quinolone derivatives as new anticancer candidates (9). These derivatives can act as anti-mitotic agents by inhibiting tubulin polymerization and disrupting microtubule organization (9,11). Previously, we demonstrated that CHM-1 (20-fluoro-6,7-methylenedioxy-2-phenyl-4-quinolone) induced DNA damage and inhibited the expression of DNA repair genes in human osteosarcoma U-2 OS cells (12). CHM-1 induced cell cycle arrest at the G_2/M phase and mitochondrial-dependent apoptotic cell death in CT-26 murine colorectal adenocarcinoma cells (13). Smh-3 (2-[3-(methylamino)-phenyl]-6-(pyrrolidin-1-yl) quinolin-4-one), another 2-phenyl-4-quinolone derivative, was found to induce G_2/M cell cycle arrest and mitochondria-dependent apoptotic cell death through inhibition of AKT activity in HL-60 human leukemia cells (14). In human hepatocellular carcinoma Hep3B cells, Smh-3 also induced cell cycle arrest in the G_2/M phase and apoptotic cell death through endoplasmic reticulum stress and mitochondria-dependent signaling (15). Herein, we investigated the anti-proliferative effects of 2-phenyl-4-quinolone (YT-1) (Fig. 1) on leukemia or normal cells and its underlying molecular mechanisms.

Materials and methods

Reagents and chemicals. YT-1 was provided by Professor Sheng-Chu Kuo and synthesized as previously described (10).

RPMI-1640 medium and penicillin/streptomycin were obtained from Thermo Fisher Scientific (Waltham, MA, USA). All antibodies used in this study and anti-mouse (cat. no. sc-2005) and anti-rabbit (cat. no. sc-2004) IgG peroxidase-conjugated secondary antibodies were obtained from Santa Cruz Biotechnology (Santa Cruz, CA, USA). All chemicals and reagents were purchased from Sigma-Aldrich (St. Louis, MO, USA) unless otherwise stated.

Cell culture. Human leukemia cell lines U937 (lymphoma), HL-60 (promyelocytic leukemia), K562 (chronic myeloid leukemia) and WS-1 (normal skin fetal fibroblasts) were obtained from the Bioresource Collection and Research Center (BCRC) (Hsinchu, Taiwan). All tested cells were maintained in RPMI-1640 medium supplemented with 10% fetal calf serum (HyClone Laboratories, Logan, UT, USA), 2 mM L-glutamine and antibiotics (100 U/ml penicillin and 100 μg/ml streptomycin) at 37˚C in a humidified atmosphere of 5% CO_2.

Cell viability by flow cytometry and microscopy observation. Cells were plated in a 24-well plate at a density of $2.5x10^5$ cells/ml and cultivated for 24 h in the presence of DMSO vehicle or 0.05, 0.1, 0.5, 1, 5 and 10 μM of YT-1. At each time point, cell viability was determined by propidium iodide (PI) exclusion method followed by flow cytometry (FACSCalibur flow cytometer; Becton-Dickinson, Franklin Lakes, NJ, USA) as previously described (16,17). In addition, following YT-1 treatment for 24 h, the cells were also observed and photographed by a phase-contrast microscope to monitor apoptotic characteristics before being subjected to flow cytometry.

Analysis of DNA content by flow cytometry. U937 cells ($2x10^5$ cells/well) in 12-well plates were incubated with 1 μM YT-1 for 0, 2, 4, 6, 8, 10, 12, 14, 16, 18 and 20 h. Cells were then harvested and washed twice with pre-chilled PBS. Cells were fixed in cold 70% ethanol overnight and then re-suspended in 500 μl propidium iodide (PI) staining buffer (0.1% Triton X-100, 100 μg/ml RNase A and 50 μg/ml PI in PBS) for 30 min as previously described (18,19). Analyses of cell cycle profiling and apoptotic cells were performed by flow cytometry (Becton Dickinson FACSCalibur flow cytometer) and BD CellQuest Pro software (BD Biosciences, Franklin Lakes, NJ, USA) as previously described (20-22).

Nuclear DAPI staining. After treatment with or without 1 μM YT-1 for 24 h, U937 cells ($1x10^5$ cells/well) were sequentially washed with PBS, fixed in 4% formaldehyde (Sigma-Aldrich) for 15 min and permeabilized in 0.1% Triton X-100 for 15 min. Each sample was stained with 200 μl DAPI solution (1 μg/ml) for 30 min at 37˚C in the dark. The integrity of nuclei and cells was visualized under a fluorescence microscope (Nikon, Inc., Tokyo, Japan).

DNA fragmentation assay. After treatment with 1 μM YT-1 for 24 h, U937 cells were harvested and lysed in 500 μl lysis buffer [20 mM Tris (pH 8.0), 10 mM EDTA and 0.2% Triton X-100] at 4˚C for 30 min. Cell lysates were then digested overnight with 100 μg/ml proteinase K at 50˚C followed by 1 h of 50 μg/ml RNase A incubation at 37˚C. Total DNA was extracted with phenol/chloroform/isopropanol (24:25:1) and then precipitated in 50% isopropanol. These samples were electrophoresed on 1% agarose gel in 0.5X TBE buffer. DNA was stained with 1 μg/ml ethidium bromide (EtBr) before the gel was photographed under UV light.

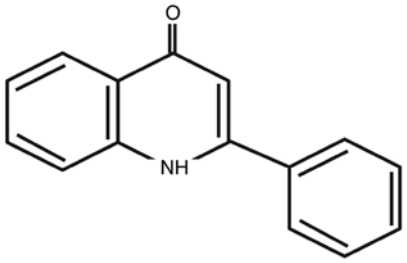

Figure 1. Chemical structure of 2-phenyl-4-quinolone (YT-1).

Annexin V/PI double staining. U937 cells ($2x10^5$ cells/well) were challenged with or without 1 μM YT-1 for 0, 3, 6, 9 and 12 h and then incubated with Annexin V and PI solution (Annexin V-FITC Apoptosis Detection kit, BD Biosciences Pharmingen, San Diego, CA, USA). According to the manufacturer's protocol, the apoptotic cells were detected by a Becton Dickinson FACSCalibur flow cytometer and quantified by BD CellQuest Pro software.

Determination of mitochondrial membrane potential ($\Delta\Psi$m) by flow cytometry. U937 cells ($2x10^5$ cell/ml) in 24-well plates were incubated with 1 μM YT-1 for 1, 2, 6, 12, 18 and 24 h. Cells were harvested, washed twice with PBS and re-suspended in 500 μl of 50 nM 3,3'-dihexyloxacarbocyanine [$DiOC_6(3)$] solution (Thermo Fisher Scientific) at 37˚C for 30 min. The level of $\Delta\Psi$m was determined and quantified by flow cytometry (Becton Dickinson FACSCalibur flow cytometer).

Western blot analysis. U937 cells ($1x10^7$ cells) were plated in 75-T flasks in the presence of 1 μM YT-1 for 2, 4, 6, 8, 10, 12 and 18 h. Cell pellets were re-suspended in ice-cold lysis buffer (150 mM sodium chloride, 1.0% NP-40, 0.5% sodium deoxycholate, 0.1% sodium dodecyl sulfate, and 50 mM Tris, pH 8.0). Protein concentration of each cell lysate was measured by Bradford assay (Bio-Rad Laboratories, Hercules, CA, USA). Equal amount of protein from each sample (40 μg protein/lane) was resolved by 12% SDS-PAGE. The proteins were then electro-transferred onto a polyvinylidene difluoride (PVDF) membrane. The membranes were immersed in PBS/0.1% Tween-20 (PBST) containing 5% skim milk for 2 h at room temperature as previously described (20,23,24). Each blot was thereafter incubated overnight at 4˚C with the desired primary antibodies (1:1,000), including Bcl-2 (cat. no. sc-509/mouse), Bax (cat. no. sc-70405/mouse), Bak (cat. no. sc-517390/mouse), Bid (cat. no. sc-373939/mouse), cytochrome *c* (cat. no. sc-13560/mouse), caspase-3 (cat. no. sc-7272/mouse), caspase-9 (cat. no. sc-56076/mouse), PARP (cat. no. sc-7150/rabbit), cyclin A (cat. no. sc-751/rabbit), cyclin B (cat. no. sc-166210/mouse), and $p21^{CIP1/WAF1}$ (cat. no. sc-756/rabbit) and α-tubulin (cat. no. sc-5286/mouse) (all from Santa Cruz Biotechnology). Protein bands were visualized using the enhanced chemiluminescence

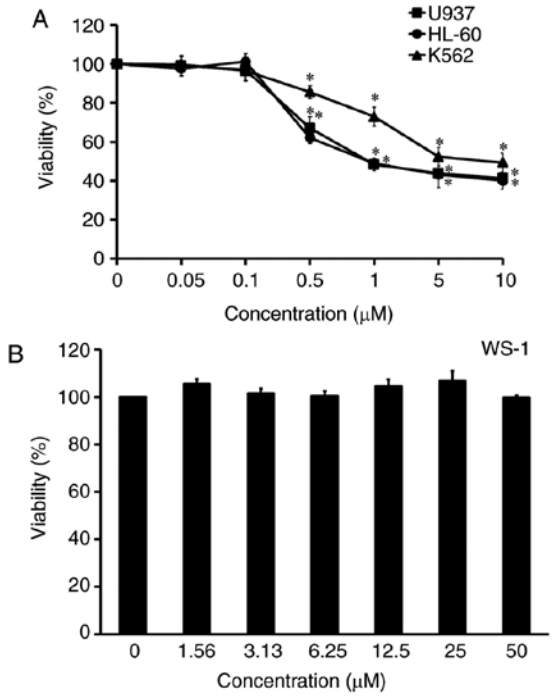

Figure 2. YT-1 is cytotoxic to human leukemia cell lines but not to human fetal skin fibroblast WS-1 cells. (A) The viability of YT-1-treated U937, HL-60 and K562 leukemia cells. (B) The viability of human skin fibroblast WS1 cells. Cells were treated with different concentrations of YT-1 for 24 h and analyzed by propidium iodide (PI) staining followed by flow cytometry. Data represent the mean ± SD (n=3); *P<0.05 and **P<0.01 vs. the YT-1-untreated control group.

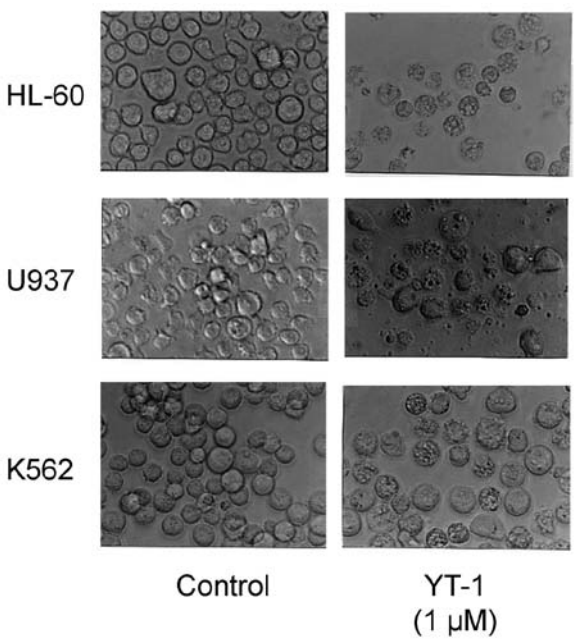

Figure 3. YT-1-induced morphological changes in U937, HL-60 and K562 leukemia cells. After exposure to 1 μM YT-1 for 24 h, cells were observed under a phase-contrast microscope and photographed. Data are representative results of three independent experiments.

(ECL) detection kit (Immobilon Western HRP Substrate, Merck Millipore, Billerica, MA, USA) and Amersham Hyperfilm ECL (GE Healthcare, Piscataway, NJ, USA). The blots were stripped and reprobed with α-tubulin as the internal loading controls.

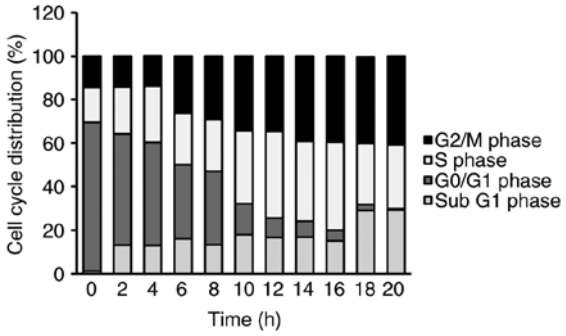

Figure 4. YT-1 induces G_2/M phase arrest and apoptosis in U937 cells. Cells were exposed to 1 μM YT-1 for the indicated periods of time and then stained with PI followed by flow cytometry. Data represent results from three independent experiments.

Statistical analysis. All data are shown as the mean ± SD (n=3). Statistical analysis of the results was carried out using the Student's t-test. P<0.05 and P<0.01 were considered statistically significant.

Results

YT-1 is cytotoxic to human leukemia cell lines but not to normal cells. The cytotoxic effect of YT-1 was examined on various human leukemia cells, including U937, HL-60 and K562 cells. After treatment with 0.05-10 μM YT-1 for 24 h, leukemia cells showed concentration-dependent sensitivity to YT-1. The IC_{50} values (the 50% inhibitory concentration of cell viability) were ~1 μM YT-1 (Fig. 2A). U937 was the most sensitive cell line to YT-1. It is worth noting that no significant cytotoxicity appeared in human fetal skin fibroblast WS-1 cells after 1.56-50 μM YT-1 challenge (Fig. 2B). Furthermore, HL-60, U937 and K562 cells following 1 μM YT-1 treatment showed morphological changes with apoptotic characteristics (cell shrinkage, rounding and membrane blebbing) (Fig. 3). We selected YT-1 at 1 μM to further investigate its effects on U937 cells.

YT-1 induces G_2/M phase arrest and apoptosis in U937 cells. To investigate whether the cytotoxic effect of YT-1 was mediated by apoptotic machinery or/and interference of cell cycle distribution, the cells were exposed to 1 μM YT-1 for 2, 4, 6, 8, 10, 12, 14, 16, 18 and 20 h. We monitored the percentage of the sub-G1 population (apoptotic cells) and the cell cycle profile via PI staining followed by flow cytometry. Following 6 to 20 h of treatment, YT-1 promoted G_2/M phase arrest. It also increased the sub-G1 population (apoptotic cells) after a 2-h exposure (Fig. 4). In addition, results from DAPI staining showed that YT-1 caused an increase in the fluorescence intensity in nuclei and apoptotic bodies (Fig. 5A). These results indicated that YT-1 caused chromatin condensation and cleavage of nuclei in the U937 cells. In addition, YT-1 treatment at 1, 10 and 25 μM concentrations provoked inter-nucleosomal DNA fragmentation in the U937 cells (Fig. 5B). At indicated intervals of time, YT-1 triggered a concentration-dependent increase in Annexin-positive/PI-negative (Annexin V^+/PI^-) cell population, which is the cell population with early signs of apoptosis. Approximately 11% of the U937 cells were Annexin V^+/PI^- visualized at a 12-h exposure (Fig. 6). Based on these findings,

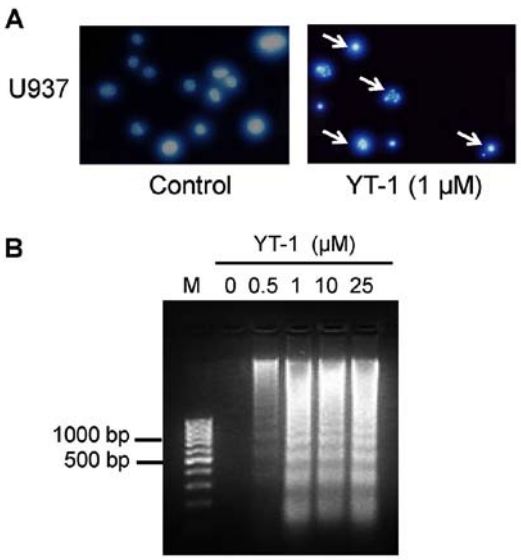

Figure 5. YT-1 triggers apoptosis and DNA fragmentation in U937 cells. Cells were incubated in the presence of different concentrations of YT-1 for 24 h. (A) DAPI staining was used to analyze apoptotic bodies in the YT-1-treated U937 cells. (B) DNA ladders were analyzed by agarose gel electrophoresis in U937 cells after different concentrations of YT-1. Data are representative results of three independent experiments.

the cytotoxic impact of YT-1 might result from G_2/M phase arrest and apoptotic death in U937 cells.

YT-1 disrupts the mitochondrial membrane potential (ΔΨm) in U937 cells. To explore whether the apoptosis induced by YT-1 was mediated by the mitochondrial pathway, we detected alterations in ΔΨm. YT-1-treated U937 cells were analyzed by $DiOC_6(3)$ incorporation. The resulting flow cytometric profile exhibited a left-shifted fluorescent peak. Following 24 h of 1 μM YT-1 treatment, the loss of ΔΨm increased from 12.1 to 78.7%. The time-dependent loss of ΔΨm indicated that YT-1-induced apoptosis was mediated through mitochondrial regulation in U937 cells.

YT-1 triggers mitochondria-mediated apoptosis in U937 cells. We next determined the effects of YT-1 on Bcl-2 family-regulated molecules and intrinsic caspase activation in U937 cells by western blotting. The results demonstrated that the protein levels of Bax and Bak were increased, while those of Bcl-2 and Bid were decreased in a time-dependent manner (Fig. 8). Moreover, YT-1 increased the expression of cytochrome *c* and proteolytically activated caspase-3 and caspase-9 after exposure to 1 μM YT-1 (Fig. 8). These findings revealed that mitochondria-dependent intrinsic apoptosis signaling was involved in the YT-1-triggered U937 cell death.

Discussion

Previously we designed and synthesized 2-phenyl-4-quinolone derivatives to screen potential anti-inflammatory and anticancer compounds (9,11-15). In the present study, we investigated 2-phenyl-4-quinolone (YT-1) for its effects on anti-leukemia activity and signaling transduction associated with G_2/M

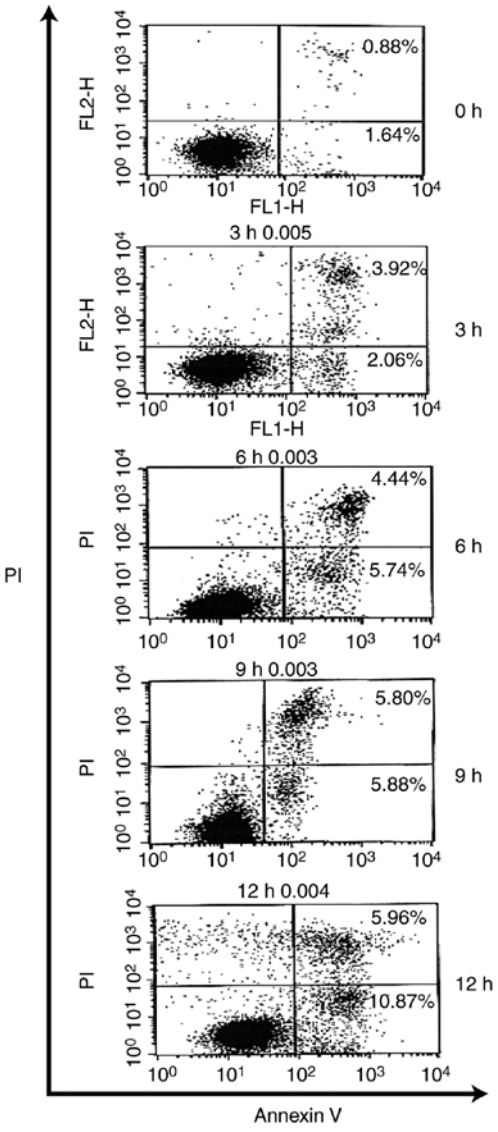

Figure 6. YT-1 promotes early apoptosis in U937 cells. Apoptosis in U937 cells was assessed at 0, 3, 6, 9, and 12 h after exposure to 1 μM YT-1 by Annexin V-FITC/PI assay followed by flow cytometry. Apoptotic cell numbers show the percentage of Annexin V^+/PI^- and Annexin V^-/PI^- cells in each quadrant. Data are representative results of three independent experiments.

arrest and apoptosis in leukemia cell lines. YT-1 significantly inhibited the cell proliferation of U937, HL-60 and K562 cells (Fig. 2A). Importantly, YT-1 had only a weak cytotoxic effect on normal human skin fibroblast WS-1 cells when compared with its effect on U937, HL-60 and K562 cells (Fig. 2B).

Wang *et al* (25) showed that YT-1 inhibits neutrophil $O_2^{\cdot-}$ generation *in vitro*. YT-1 increased cellular cyclic AMP levels by inhibiting phosphodiesterase (PDE) activity in formyl-methionyl-leucyl-phenylalanine (fMLP)-induced respiratory burst in rat neutrophils, with an IC_{50} value of 60.7±8.2 μM. Kuo *et al* (10) demonstrated that 2-phenyl-4-quinolone derivatives have significant cytotoxic effects against human lung carcinoma (A-549), ileocecal carcinoma (HCT-8), melanoma (RPMI-7951), epidermoid carcinoma of the nasopharynx (KB) and two murine leukemia cell lines (P-388 and L1210). We selected a dosage of 1 μM of lead compound YT-1 to investigate its molecular mechanisms underlying its anti-leukemia activity *in vitro*. The results are summarized as follows. i) In

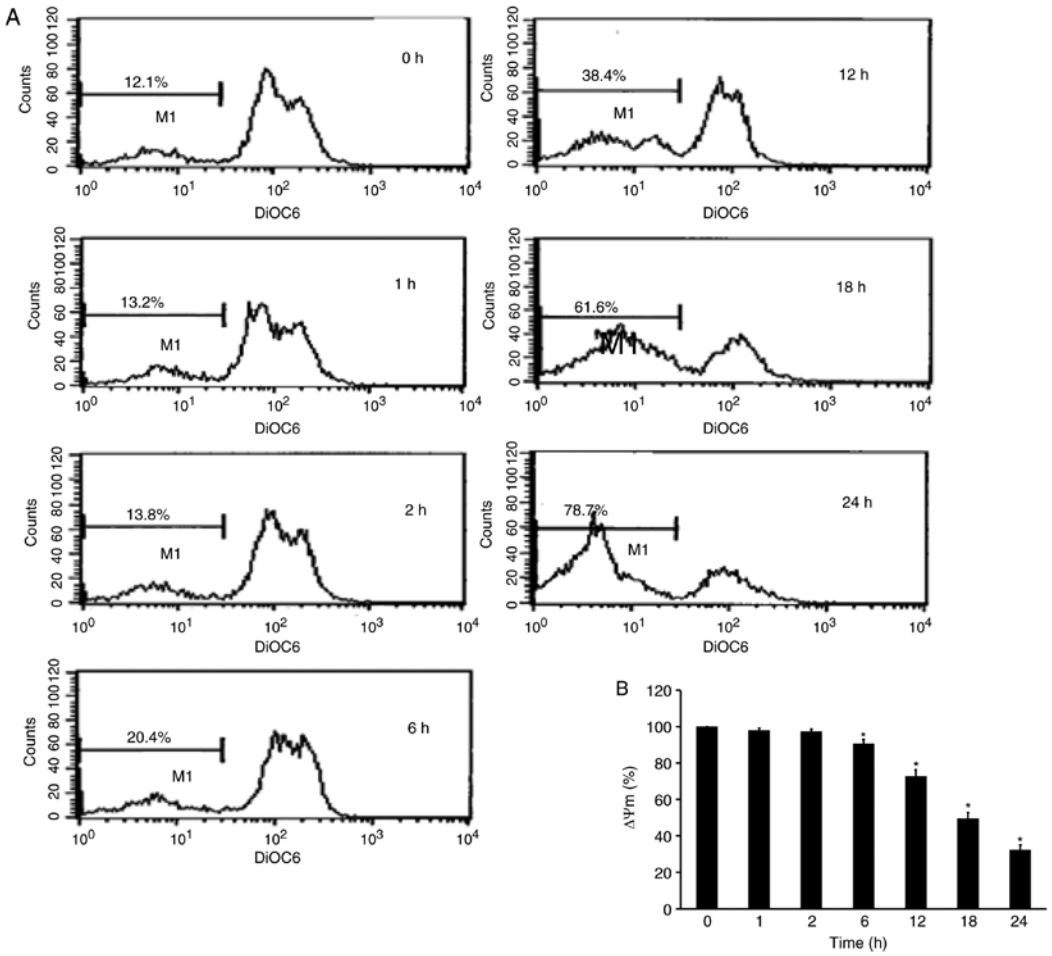

Figure 7. YT-1 stimulates the disruption of the mitochondrial membrane potential (ΔΨm) in U937 cells. (A) Cells were treated with 1 μM YT-1 for the indicated lengths of time and then probed with $DiOC_6(3)$ by flow cytometry. (B) Quantitation of the data for ΔΨm as detected by flow cytometric analysis. Data represent the mean ± SD (n=3); $^*P<0.05$ vs. the YT-1-untreated control group.

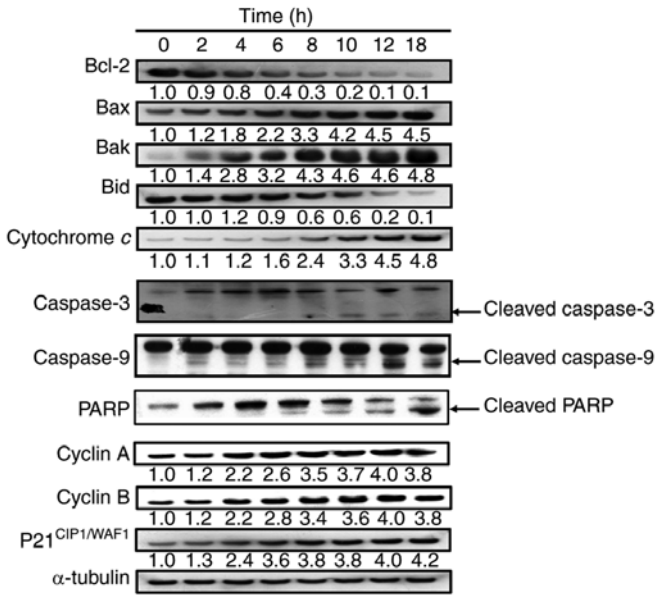

Figure 8. YT-1 alters expression of the Bcl-2 family and mitochondria-dependent proteins in U937 cells. Cells were incubated with 1 μM YT-1 for the indicated lengths of time. Cell lysates were collected and blotted with antibodies for mitochondria-regulated signals (Bcl-2, Bax, Bak, Bid, cytochrome c, caspase-3, caspase-9, PARP, cyclin A, cyclin B, and $p21^{CIP1/WAF1}$). α-tubulin was used as the internal control.

HL-60, U937 and K562 cells, 6-20 h of YT-1 treatment caused growth inhibition (Fig. 2A) and cell cycle arrest at the G_2/M phase (Fig. 4). ii) YT-1 increased protein levels of cyclin A, cyclin B and CDK1 in U937 cells (Fig. 8). iii) YT-1 induced apoptotic body formation (Fig. 3), chromatin condensation (Fig. 5A), and DNA fragmentation (Fig. 5B) in U937 cells (Fig. 8). iv) YT-1 induced early apoptosis as demonstrated by increased Annexin V-positive U937 cells (Fig. 6). v) YT-1 decreased the mitochondrial membrane potential in U937 cells (Fig. 7). vi) YT-1 caused a decrease in the protein level of Bcl-2 and Bid, but increased the protein levels of Bax and Bak in U937 cells (Fig. 8). vii) YT-1 increased protein levels of cleaved-activated caspase-3 and caspase-9 and the cleaved form of PARP in U937 cells. Based on these results, we suggest that YT-1 induced apoptotic cell death through the mitochondria-dependent pathway in U937 cells.

2-Phenyl-4-quinolone derivatives are potent inhibitors of tubulin polymerization (9,11). These activities are nearly comparable to those of the anti-mitotic natural products colchicine, podophyllotoxin, and combretastatin A-4 (26,27). Previous studies indicate that microtubule-targeting agents (MTAs) promote CDK1 activity (28-30). CDK1 plays a pro-apoptotic role in microtubule-targeting agents (27). An increase in CDK1 activity and induction of apoptosis have been demonstrated by paclitaxel (Taxol) and vinca alkaloids

(vinblastine, vincristine) in leukemia cells (27,31). CDK1 can trigger mitochondrial membrane permeabilization by targeting anti-apoptotic Bcl-2 protein (27). Bcl-2 protein was phosphorylated by CDK1 on Ser70 and was found to suppress its anti-apoptotic activity, therefore leading to apoptosis (12). As to the G_2/M arrest induction by YT-1 (Fig. 4), our results further demonstrated that YT-1 increased protein levels of $p21^{CIP1/WAF1}$, cyclin A, cyclin B and CDK1 (Fig. 8) in U937 cells. We suggest that YT-1 causes cell cycle arrest at the G_2/M phase and apoptosis through CDK1-mediated Bcl-2 phosphorylation.

Once anticancer drugs trigger mitochondria-dependent apoptotic pathways, the mitochondrial outer membrane becomes permeable, and then cytochrome *c*, Apaf-1, pro-caspase-9, AIF and Endo G are released into the cytosol to sequentially activate caspase-9 and caspase-3, eventually leading to apoptotic cell death (16,17,32). YT-1 decreased the mitochondrial membrane potential (Fig. 7), and reduced Bcl-2 and Bid protein levels. In contrast, YT-1 upregulated Bax and Bak, activated caspase-3 and caspase-9, and increased the proteolytic cleavage of PARP in U937 cells (Fig. 8). The results revealed that YT-1 triggers an mitochondria-dependent apoptotic mechanism (an intrinsic pathway).

In conclusion, YT-1 showed significant cytotoxicity against HL-60, U937 and K562 leukemia cells. However, YT-1 was less toxic to normal human skin fibroblast WS-1 cells. The mechanisms underlying the inhibitory effects of YT-1 in U937 human leukemia cells included the promotion of G_2/M phase arrest and induction of the mitochondria-dependent apoptotic pathway.

Acknowledgements

This research was supported by a grant (CTCN-104-08) from the Cardinal Tien Junior College of Healthcare and Management (New Taipei, Taiwan).

References

1. Kohnken R, Porcu P and Mishra A: Overview of the use of murine models in leukemia and lymphoma research. Front Oncol 7: 22, 2017.
2. Allart-Vorelli P, Porro B, Baguet F, Michel A and Cousson-Gélie F: Haematological cancer and quality of life: A systematic literature review. Blood Cancer J 5: e305, 2015.
3. Medinger M, Zeiter D, Heim D, Halter J, Gerull S, Tichelli A, Passweg J and Nigro N: Hypothyroidism following allogeneic hematopoietic stem cell transplantation for acute myeloid leukemia. Leuk Res 58: 43-47, 2017.
4. Murakami K, Kohashi S, Sakurai M, Kato J, Toyama T, Koda Y, Yamane Y, Hashida R, Abe R, Yamazaki R, *et al*: Hyponatremia associated with human herpesvirus-6 (HHV-6) encephalitis after allogeneic hematopoietic stem cell transplantation: A presentation different from HHV-6 myelitis. Int J Hematol: May 13, 2017 (Epub ahead of print).
5. Tanoue S, Konuma T, Takahashi S, Watanabe E, Sato N, Watanabe N, Isobe M, Kato S, Ooi J and Tojo A: Long-term persistent donor-recipient mixed chimerism without disease recurrence after myeloablative single-unit cord blood transplantation in adult acute myeloid leukemia following myelodysplastic syndrome. Leuk Lymphoma 54: 2973-2975, 2017.
6. Busca A, Lessi F, Verga L, Candoni A, Cattaneo C, Cesaro S, Dragonetti G, Delia M, De Luca A, Guglielmi G, *et al*: SEIFEM 2010-E: Economic evaluation of posaconazole for antifungal prophylaxis in patients with acute myeloid leukemia receiving induction chemotherapy. Leuk Lymphoma 58: 2859-2864, 2017.
7. Hour MJ, Huang LJ, Kuo SC, Xia Y, Bastow K, Nakanishi Y, Hamel E and Lee KH: 6-Alkylamino- and 2,3-dihydro-3'-methoxy-2-phenyl-4-quinazolinones and related compounds: Their synthesis, cytotoxicity, and inhibition of tubulin polymerization. J Med Chem 43: 4479-4487, 2000.
8. Xia Y, Yang ZY, Xia P, Bastow KF, Tachibana Y, Kuo SC, Hamel E, Hackl T and Lee KH: Antitumor agents. 181. Synthesis and biological evaluation of 6,7,2',3',4'-substituted-1,2,3,4-tetrahydro-2-phenyl-4-quinolones as a new class of antimitotic antitumor agents. J Med Chem 41: 1155-1162, 1998.
9. Li L, Wang HK, Kuo SC, Wu TS, Mauger A, Lin CM, Hamel E and Lee KH: Antitumor agents. 155. Synthesis and biological evaluation of 3',6,7-substituted 2-phenyl-4-quinolones as antimicrotubule agents. J Med Chem 37: 3400-3407, 1994.
10. Kuo SC, Lee HZ, Juang JP, Lin YT, Wu TS, Chang JJ, Lednicer D, Paull KD, Lin CM, Hamel E, *et al*: Synthesis and cytotoxicity of 1,6,7,8-substituted 2-(4'-substituted phenyl)-4-quinolones and related compounds: Identification as antimitotic agents interacting with tubulin. J Med Chem 36: 1146-1156, 1993.
11. Hsu SC, Yang JS, Kuo CL, Lo C, Lin JP, Hsia TC, Lin JJ, Lai KC, Kuo HM, Huang LJ, *et al*: Novel quinolone CHM-1 induces apoptosis and inhibits metastasis in a human osterogenic sarcoma cell line. J Orthop Res 27: 1637-1644, 2009.
12. Chen HY, Lu HF, Yang JS, Kuo SC, Lo C, Yang MD, Chiu TH, Chueh FS, Ho HC, Ko YC and Chung JG: The novel quinolone CHM-1 induces DNA damage and inhibits DNA repair gene expressions in a human osterogenic sarcoma cell line. Anticancer Res 30: 4187-4192, 2010.
13. Chou LC, Yang JS, Huang LJ, Wu HC, Lu CC, Chiang JH, Chen KT, Kuo SC and Chung JG: The synthesized 2-(2-fluorophenyl)-6,7-methylenedioxyquinolin-4-one (CHM-1) promoted G2/M arrest through inhibition of CDK1 and induced apoptosis through the mitochondrial-dependent pathway in CT-26 murine colorectal adenocarcinoma cells. J Gastroenterol 44: 1055-1063, 2009.
14. Huang SM, Yang JS, Tsai SC, Chen MH, Hsu MH, Lin HY, Chou LC, Chinag JH, Lee KH, Huang LJ and Kuo SC: The novel synthesized 2-(3-(methylamino)phenyl)-6-(pyrrolidin-1-yl) quinolin-4-one (Smh-3) compound induces G2/M phase arrest and mitochondrial-dependent apoptotic cell death through inhibition of CDK1 and AKT activity in HL-60 human leukemia cells. Int J Oncol 38: 1357-1364, 2011.
15. Liu CY, Yang JS, Huang SM, Chiang JH, Chen MH, Huang LJ, Ha HY, Fushiya S and Kuo SC: Smh-3 induces G(2)/M arrest and apoptosis through calciummediated endoplasmic reticulum stress and mitochondrial signaling in human hepatocellular carcinoma Hep3B cells. Oncol Rep 29: 751-762, 2013.
16. Lu CC, Yang JS, Huang AC, Hsia TC, Chou ST, Kuo CL, Lu HF, Lee TH, Wood WG and Chung JG: Chrysophanol induces necrosis through the production of ROS and alteration of ATP levels in J5 human liver cancer cells. Mol Nutr Food Res 54: 967-976, 2010.
17. Chiang JH, Yang JS, Ma CY, Yang MD, Huang HY, Hsia TC, Kuo HM, Wu PP, Lee TH and Chung JG: Danthron, an anthraquinone derivative, induces DNA damage and caspase cascades-mediated apoptosis in SNU-1 human gastric cancer cells through mitochondrial permeability transition pores and Bax-triggered pathways. Chem Res Toxicol 24: 20-29, 2011.
18. Chiu YJ, Hour MJ, Lu CC, Chung JG, Kuo SC, Huang WW, Chen HJ, Jin YA and Yang JS: Novel quinazoline HMJ-30 induces U-2 OS human osteogenic sarcoma cell apoptosis through induction of oxidative stress and up-regulation of ATM/p53 signaling pathway. J Orthop Res 29: 1448-1456, 2011.
19. Yang JS, Hour MJ, Kuo SC, Huang LJ and Lee MR: Selective induction of G2/M arrest and apoptosis in HL-60 by a potent anticancer agent, HMJ-38. Anticancer Res 24: 1769-1778, 2004.
20. Lin CF, Yang JS, Lin C, Tsai FJ, Lu CC and Lee MR: CCY-1a-E2 induces G2/M phase arrest and apoptotic cell death in HL-60 leukemia cells through cyclin-dependent kinase 1 signaling and the mitochondria-dependent caspase pathway. Oncol Rep 36: 1633-1639, 2016.
21. Chen YF, Yang JS, Chang WS, Tsai SC, Peng SF and Zhou YR: Houttuynia cordata Thunb extract modulates G0/G1 arrest and Fas/CD95-mediated death receptor apoptotic cell death in human lung cancer A549 cells. J Biomed Sci 20: 18, 2013.
22. Wu SH, Hang LW, Yang JS, Chen HY, Lin HY, Chiang JH, Lu CC, Yang JL, Lai TY, Ko YC and Chung JG: Curcumin induces apoptosis in human non-small cell lung cancer NCI-H460 cells through ER stress and caspase cascade- and mitochondria-dependent pathways. Anticancer Res 30: 2125-2133, 2010.

23. Lai KC, Lu CC, Tang YJ, Chiang JH, Kuo DH, Chen FA, Chen IL and Yang JS: Allyl isothiocyanate inhibits cell metastasis through suppression of the MAPK pathways in epidermal growth factor-stimulated HT29 human colorectal adenocarcinoma cells. Oncol Rep 31: 189-196, 2014.
24. Ma YS, Weng SW, Lin MW, Lu CC, Chiang JH, Yang JS, Lai KC, Lin JP, Tang NY, Lin JG and Chung JG: Antitumor effects of emodin on LS1034 human colon cancer cells in vitro and in vivo: Roles of apoptotic cell death and LS1034 tumor xenografts model. Food Chem Toxicol 50: 1271-1278, 2012.
25. Wang JP, Raung SL, Huang LJ and Kuo SC: Involvement of cyclic AMP generation in the inhibition of respiratory burst by 2-phenyl-4-quinolone (YT-1) in rat neutrophils. Biochem Pharmacol 56: 1505-1514, 1998.
26. Lu CC, Yang JS, Chiang JH, Hour MJ, Lin KL, Lin JJ, Huang WW, Tsuzuki M, Lee TH and Chung JG: Novel quinazolinone MJ-29 triggers endoplasmic reticulum stress and intrinsic apoptosis in murine leukemia WEHI-3 cells and inhibits leukemic mice. PLoS One 7: e36831, 2012.
27. Yang JS, Hour MJ, Huang WW, Lin KL, Kuo SC and Chung JG: MJ-29 inhibits tubulin polymerization, induces mitotic arrest, and triggers apoptosis via cyclin-dependent kinase 1-mediated Bcl-2 phosphorylation in human leukemia U937 cells. J Pharmacol Exp Ther 334: 477-488, 2010.
28. Chan KS, Koh CG and Li HY: Mitosis-targeted anti-cancer therapies: Where they stand. Cell Death Dis 3: e411, 2012.
29. Lu CC, Yang JS, Chiang JH, Hour MJ, Lin KL, Lee TH and Chung JG: Cell death caused by quinazolinone HMJ-38 challenge in oral carcinoma CAL 27 cells: Dissections of endoplasmic reticulum stress, mitochondrial dysfunction and tumor xenografts. Biochim Biophys Acta 1840: 2310-2320, 2014.
30. Chiang JH, Yang JS, Lu CC, Hour MJ, Chang SJ, Lee TH and Chung JG: Newly synthesized quinazolinone HMJ-38 suppresses angiogenetic responses and triggers human umbilical vein endothelial cell apoptosis through p53-modulated Fas/death receptor signaling. Toxicol Appl Pharmacol 269: 150-162, 2013.
31. Bates D, Feris EJ, Danilov AV and Eastman A: Rapid induction of apoptosis in chronic lymphocytic leukemia cells by the microtubule disrupting agent BNC105. Cancer Biol Ther 17: 291-299, 2016.
32. Lu CC, Huang BR, Liao PJ and Yen GC: Ursolic acid triggers nonprogrammed death (necrosis) in human glioblastoma multiforme DBTRG-05MG cells through MPT pore opening and ATP decline. Mol Nutr Food Res 58: 2146-2156, 2014.